Robotica (2001) volume 19, pp. 275–284. Printed in the United Kingdom © 2001 Cambridge University Press

A 3D passive dynamic biped with yaw and roll compensation

M. Wisse*, A. L. Schwab**, R. Q. vd. Linde*

**Man-Machine Systems and Control, **Laboratory for Engineering Mechanics, Delft University of Technology, Mekelweg 2, NL-2628 CD Delft, The Netherlands. E-mail: m.wisse@wbmt.tudelft.nl*

(Received in Final Form: August 11, 2000)

SUMMARY

Autonomous walking bipedal machines, possibly useful for rehabilitation and entertainment purposes, need a high energy efficiency, offered by the concept of 'Passive Dynamic Walking' (exploitation of the natural dynamics of the robot). 2D passive dynamic bipeds have been shown to be inherently stable, but in the third dimension two problematic degrees of freedom are introduced: yaw and roll.

We propose a design for a 3D biped with a pelvic body as a passive dynamic compensator, which will compensate for the undesired yaw and roll motion, and allow the rest of the robot to move as if it were a 2D machine. To test our design, we perform numerical simulations on a multibody model of the robot. With limit cycle analysis we calculate the stability of the robot when walking at its natural speed.

The simulation shows that the compensator, indeed, effectively compensates for both the yaw and the roll motion, and that the walker is stable.

KEYWORDS: Passive dynamic walking; Biped; Dynamic; Yaw; Efficient

1. INTRODUCTION

1.1 Passive Dynamic Walking

In the past few decades robotics research has made huge progress in the area of biped locomotion for various reasons, running from prosthesis development to entertainment industries. Several institutions have succeeded in building successful walking bipeds. One of the under-addressed problems is energy consumption. Most existing bipeds need an 'umbilical cord' for power supply. Honda Motor Co.[1] developed a completely autonomous humanoid robot, but it has to carry 20 kilograms of batteries for a 15 minute walk!

A solution for energy efficiency is the exploitation of the 'natural dynamics' of the multi-body system. In 1989 McGeer[2] introduced the idea of 'passive dynamic walking', inspired by the research of Mochon and McMahon.[3] They showed that in human locomotion the motion of the swing leg is merely a result of gravity acting on an unactuated double pendulum. McGeer extended the idea and showed that a completely unactuated and therefore *uncontrolled* robot can perform a stable walk. Garcia *et al.*[4] have researched several stability and efficiency issues of those passive dynamic walkers, and showed that in the limiting case, energy consumption can even be reduced to zero, like an ideal rolling wheel.

The walking motion of a passive dynamic walker is started by launching the robot with such initial values for the leg angles and velocities, that the end of that stride (the beginning of a new stride) is nearly identical to that in the starting conditions. A periodic or cyclic walking motion will then result. At each stride, when the heel strikes the floor, the impact will result in a loss of energy. This loss can be compensated for by having the robot walk down a shallow slope, or by periodically supplying energy with an actuator.

A passive dynamic walker has no controls, therefore it has to be inherently stable. Although the stance leg is an inverted pendulum so that the walker is statically unstable when standing, surprisingly a passive dynamic walker can possess stability when walking. This dynamic stability of the cyclic walking motion depends on the values of the design parameters (such as mass distribution). Before a prototype can be designed, the proper values for the design parameters should be determined. Therefore, a stability analysis of a model of the prospective prototype will be performed with the aid of numerical simulations.

1.2 Current research status

Walking toys that are based on the 'passive dynamic'-principle have already existed for more than a hundred years.[5] McGeer started a more systematic research of these walkers. His most advanced prototype[6] is a 2D passive dynamic walker with knees (see Fig. 1). It achieves a (near-)2D-behaviour with two pairs of legs: One outer pair and one inner pair.

Coleman[7] built a 3D passive dynamic walker with straight legs (Fig. 2). The prototype proved to be marginally stable by virtue of a non-anthropomorphic mass distribution.

Van der Linde[8] built an internally powered 3D passive dynamic walker (Fig. 3). The energy is supplied by small actuators periodically extending the legs.

Wisse and Ruina constructed a 3D kneed passive dynamic walker based on 2D simulations (Fig. 4). As with Coleman's straight legged 3D walker, there was only marginal stability.

1.3 Goal of research

In order to make the concept of Passive Dynamic Walking applicable for prosthetics research or entertainment purposes, we want to go towards a more anthropomorphic leg design. We aim to combine all three anthropomorphic

https://doi.org/10.1017/S0263574700003040 Published online by Cambridge University Press

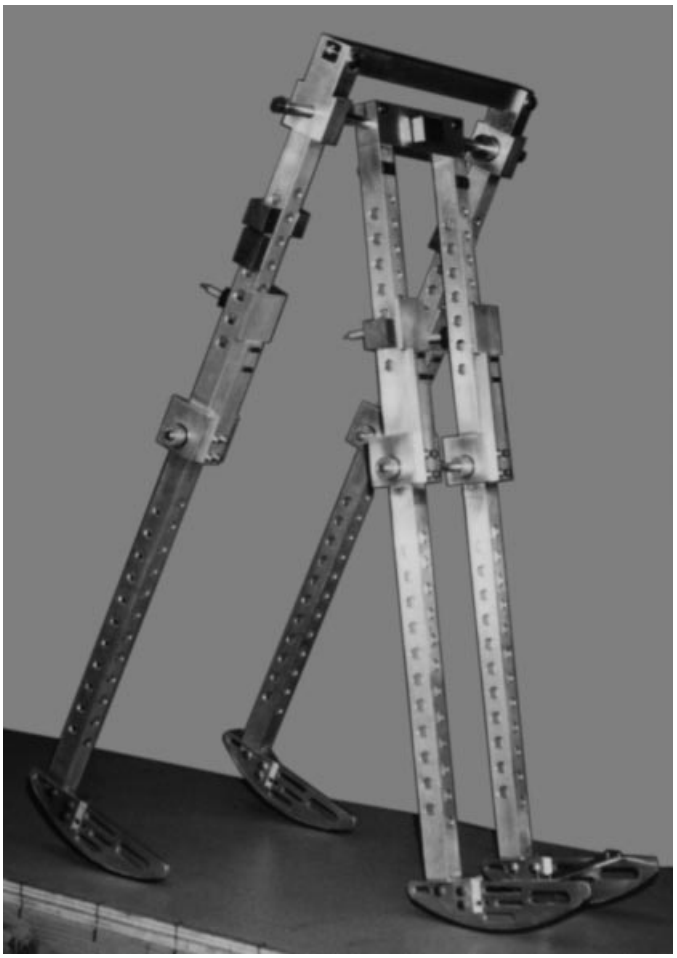


Fig. 1. Close copy of McGeer's prototype of a kneed 2D walker, by Garcia *et al.*[4]

characteristics of the previously mentioned prototypes into one new 3D robot, i.e.

- two legs
- actuation
- knees

Up till now no passive dynamic walker exists with an upper body. Our design will involve the introduction of a 'pelvic body'. This is not meant as an anthropomorphic upper body, but as a means for compensating for undesired 3D motions.

Before we start designing and building the actual prototype, we want to analyze the stability of the prospective prototype by a simulation of the dynamic behaviour. In contrast with the ample stability of 2D simulations and prototypes, we know of only few other stable 3D models.[9] The problematic degrees of freedom are yaw, rotation around a vertical axis, and roll, tipping over sideways. We want to extend the walker with a pelvic body, aiming to compensate for those degrees of freedom. This will allow the legs to remain in the sagittal plane, and their motion will resemble that of a 2D walker. This paper describes the simulations performed on a 3D model with knees, ankles, and a pelvic compensator body, to answer the questions:

- Is compensation of yaw and roll possible with a passive dynamic compensator?
- Will this design result in stable walking behaviour?

2. MODEL

In this section we will describe our computer model necessary for stability analysis. It is a passive dynamic walker with two legs with knees and actuated ankles, and a pelvic compensator body (see Fig. 5). The model has 9 degrees of freedom (see Fig. 6). Some of the model elements are already known from McGeer[6] and Garcia[4], like the 2D passive dynamic walking behavior and the passive knees. We introduce actuated ankles for walking on level ground, a foot contact model allowing yaw, and a pelvic body meant to compensate for the undesired out-of plane motions (yaw and roll).

2.1 Basic passive dynamic walker

The basic passive dynamic walker is McGeer's 2D straight legged walker[2] (see Fig. 7). This walker has two equal legs, modeled as rigid bodies coupled with a frictionless hinge at the hip. A stride begins when one leg leaves the floor, and

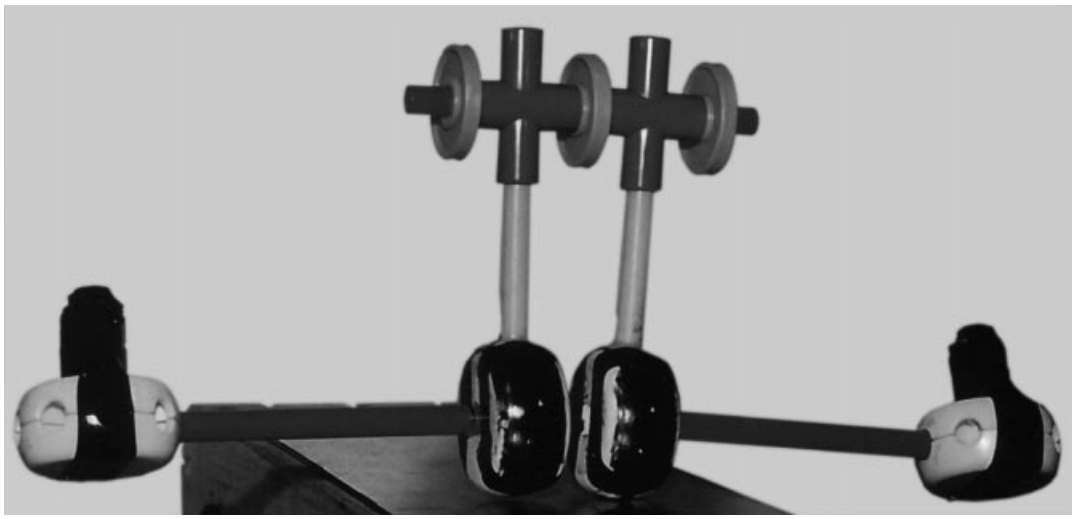


Fig. 2. Coleman's[7] prototype of a straight legged 3D walker, constructed with TinkerToys™.

https://doi.org/10.1017/S0263574700003040 Published online by Cambridge University Press

ends just after ‘heel strike’, when the other leg is bound to leave the floor. At heel strike, the impact is assumed to be fully inelastic, and the other foot is leaving the ground at that instant, since there is no leg compliance. Therefore, at all times there is exactly one foot in contact with the floor. To compensate for the energy loss at heel strike, the robot walks down a shallow slope.

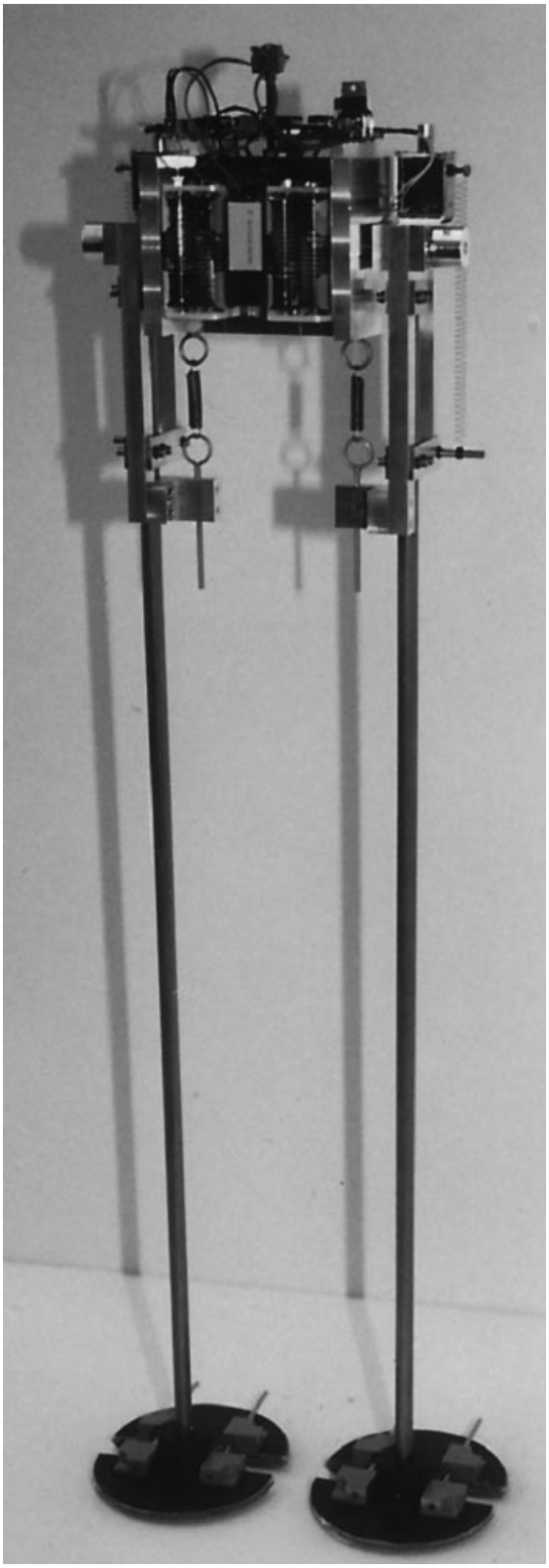


Fig. 3. Van der Linde’s[8] powered straight legged 2D walker.

2.2 Knees and ankles

The knee is modeled as a passive hinge with a unilateral constraint, which prevents the knee from hyper-extension. Similar to McGeer’s kneed model and prototype, impacts into this bump stop are assumed to be fully inelastic. After a full knee extension has been reached the thigh and shank are assumed to be rigidly connected throughout the rest of the stride.

To remove the necessity for walking downhill, Van der Linde proposed periodic actuation by extension of the legs.[10] We use the same principle of adding energy at some instant during every stride, but take a more anthropomorphic approach. Our model has lightweight, flat feet mounted on periodically actuated ankle joints. The actuator is connected to the heel by a string (see Fig. 8). If the string is stretched, the actuator can extend the ankle joint. Otherwise, the ankle behaves as a free joint. This behavior is comparable to a stretch reflex without time delay.

In our model we assume that the feet are weightless, and that the instant of heel strike is determined by a zero vertical distance between the floor and the swing leg ankle.

2.3 Yaw

Counterswinging legs give a variation in angular momentum around the vertical axis. This can be easily

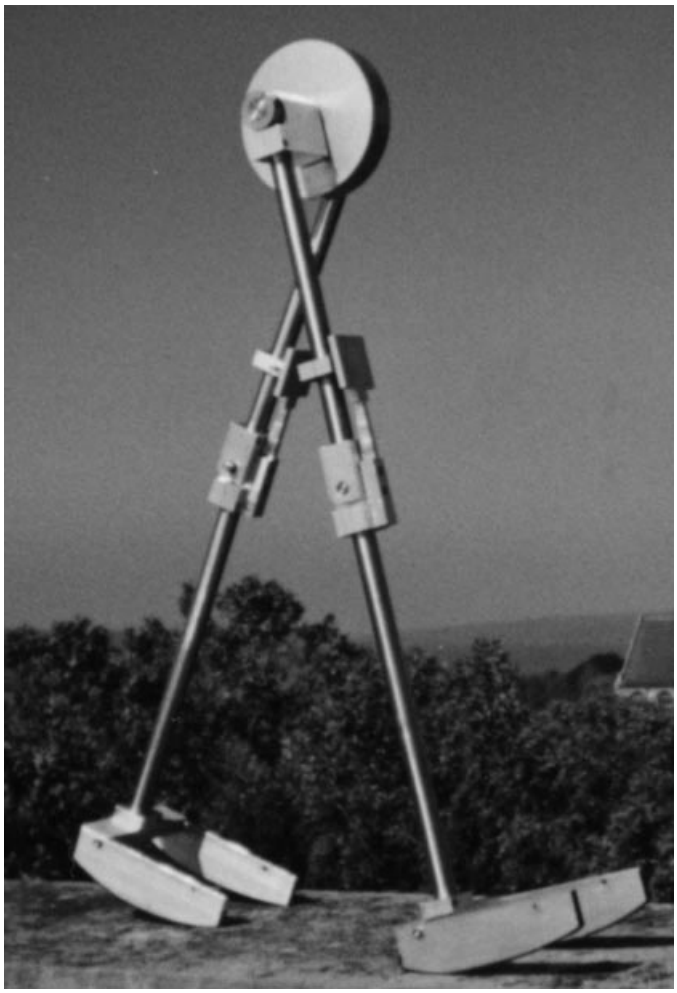


Fig. 4. Anthropomorphic passive dynamic walker by Wisse and Ruina [unpublished] at Cornell University, USA, 1998.

https://doi.org/10.1017/S0263574700003040 Published online by Cambridge University Press

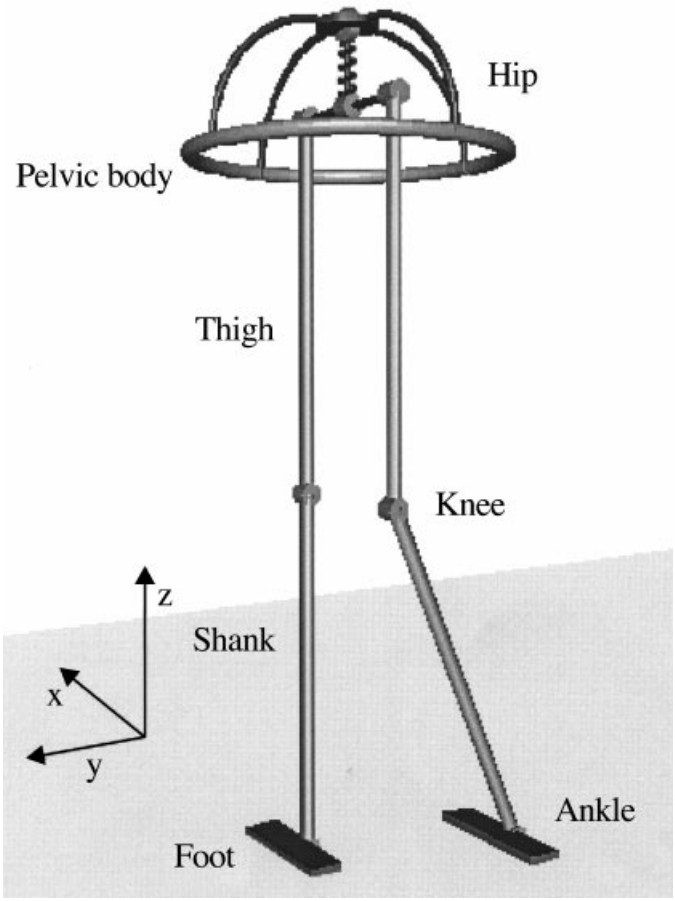


Fig. 5. Rendered view of our 3D biped model.

demonstrated with two pendulums mounted on a horizontal axle that is suspended from the ceiling by a cord. Releasing the pendulums in opposite directions results in a counter-swinging motion, while the system as a whole oscillates around the vertical axis (the cord).

From experience with other 3D prototypes[7,8] we know that contact between the stance foot and the floor is not perfect. While friction between the foot and floor is large enough to prevent forward or sideways slip, it is not always capable of sufficient torsional resistance. Therefore, during a stride the robot will rotate around a vertical axis going through the stance foot. In a prototype, the center of rotation will not be a fixed point; it depends on the continuously changing pressure distribution over the contact area of the foot. The dynamic model of the contact between stance foot and floor is a complex contact problem. For the sake of simplicity, we assume that the center of rotation lies in the center of the stance foot. This leads to a foot contact model according to Fig. 6. Dynamic friction between the rotating foot and the floor is modeled as linear damping.

The tendency to yaw is disastrous for the stability of the walking motion. To bring the motion of the legs back to 2D, we introduce a 'pelvic body' as a dynamic compensator for the yaw rotation. We mount the pelvic body on the hip-axle with a degree of freedom around the vertical axis. Applying a torsional spring between this body and the hip-axle, we obtain an oscillating body which could counteract the change in angular momentum from the legs (see Fig. 9). The success of the yaw compensation depends on the parameter

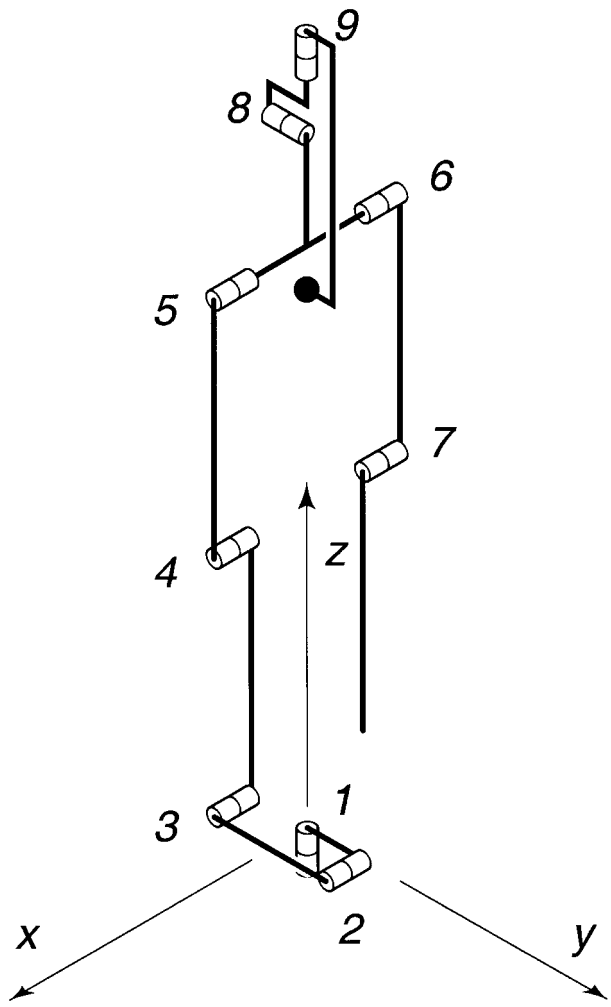


Fig. 6. Degrees of freedom of our 3D model. The massless swing foot doesn't influence the overall dynamics, and is therefore not displayed.

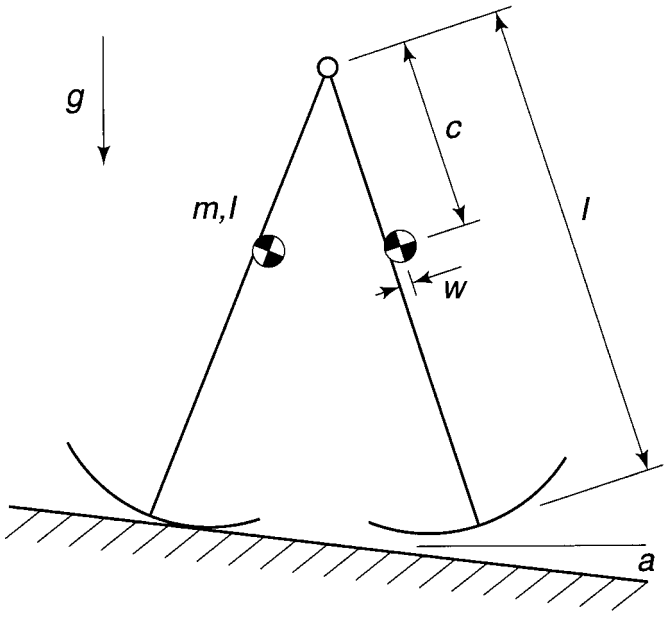


Fig. 7. Model of McGeer's straight legged 2D walker, 1989.

https://doi.org/10.1017/S0263574700003040 Published online by Cambridge University Press

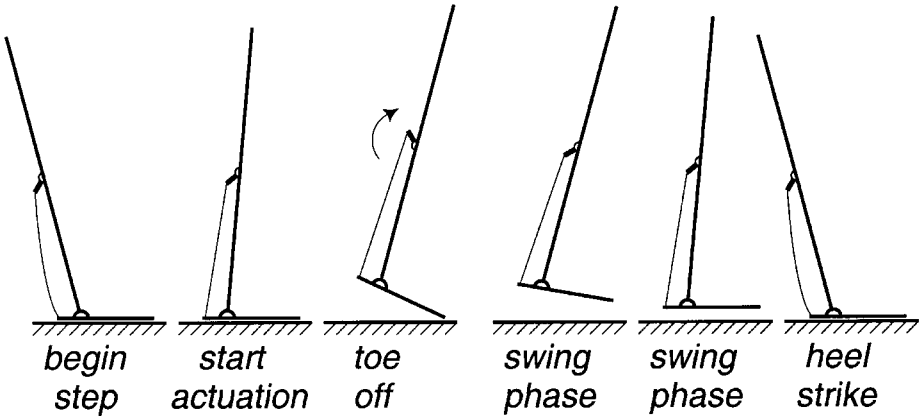


Fig. 8. Actuation scheme of ankle. During the first part of the stance phase, the ankle acts as a free joint. When the string becomes stretched, the actuator shortens the string, so that the walker rises on its toes. When the other foot hits the floor, the actuator releases the string. A small torsional spring in the ankle will keep the string stretched during the swing phase.

combination of the body and the legs together. For a good initial guess for the parameters, we bear in mind that the *eigenfrequency* of the pelvic body should be close to the oscillation frequency of the legs. If we suppose that the compensation is successful, the pelvic body acts as if it has a spring mounted on a fixed base. Therefore it will be oscillating with its *eigenfrequency.* Only if this equals the stride frequency, the compensating moment matches the required moment for the changes in angular momentum, and the premise is true. Note that the leg motions are fairly non-linear, so that the yaw compensation can never be exact with this compensator.

With the pelvic body mounted on the hip-axle, it is inevitable that it will also have a degree of freedom around this axle. However, if we situate the center of mass of the body slightly underneath this axle, it will stay more or less upright, without badly influencing the dynamics of the rest of the system.

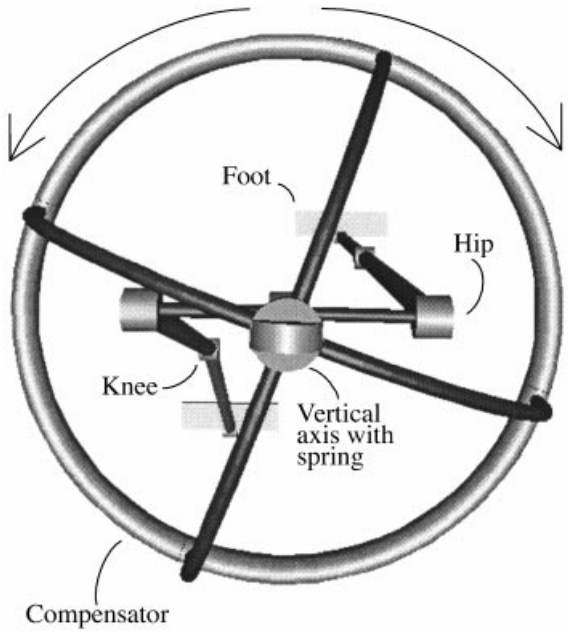


Fig. 9. Top view of our model. An oscillating compensator body counteracts the change in angular momentum from the swinging legs.

2.4 Roll

The foot contact model as shown in Fig. 6 suggests that the robot cannot tip over sideways (roll). This can only be true if the center of mass is above the alternating foot contact area, or more accurately, if the center of pressure remains within the foot contact area. There are many solutions to solve this problem, as presented by Kuo[11], one of which involves a pelvic body behaving as a pendulum in the frontal plane. Since we already have a pelvic body to compensate for the yaw motion, it is evident to use it for roll compensation as well. The motion of the pelvic body with a substantial mass accounts for the required path of the center of pressure (from one foot to the other). The *eigenfrequency* of the pelvic body in the frontal plane must be matched to the stride frequency to allow for it to be a completely passive pendulum.

Note that the foot model does not allow roll at any instance, even at heel strike. Therefore, heel strike is a fully inelastic impact of a single point (the ankle) with four impact constraints (three translations and rotation around the y-axis).

2.5 System parameters

The cyclic walking motion and its stability depend on the design parameters. Using the numerical procedures for finding cyclic motions, as described in the next section, we manually tuned the parameter combination so that a neat and stable cyclic walking motion resulted. This is not in any sense an optimized solution, but it is good enough to demonstrate that the concept of passive dynamic compensation works. Table I shows all the design parameters.

The center of mass of the shank and thigh are located on the central vertical axis through the hip, knee and ankle joint. The mass of the pelvic body is assumed to be distributed over the main ring (Fig. 5). We assume that there is no friction in any of the robot hinges, but there is damping in hinge 1 (Fig. 6) representing the foot contact with the floor.

In order to allow investigation of the 2D equivalent of our model, we have built in the possibility to fixate the 3D-degrees of freedom: yaw and roll. Results of the 2D and 3D simulations will be presented in section 4.

https://doi.org/10.1017/S0263574700003040 Published online by Cambridge University Press

Table I. Design parameters values as manually tuned to stability (See Fig. 5).

Thigh mass	0.5 [kg]
Shank mass	0.4 [kg]
Pelvic body mass	1 [kg]
Ixx Thigh	0.01 [kgm^2]
Iyy Thigh	0.01 [kgm^2]
Izz Thigh	0 [kgm^2]
Ixx Shank	0.01 [kgm^2]
Iyy Shank	0.01 [kgm^2]
Izz Shank	0 [kgm^2]
Thigh length	0.5 [m]
Shank length	0.5 [m]
Foot length	0.05 [m]
Hip width	0.2 [m]
hip-axle to pelvic axle	0.18 [m]
pelvic axle to pelvic c.m.	0.25 [m]
hip axle to thigh c.m.	0.1 [m]
knee axle to shank c.m.	0.1 [m]
pelvic ring radius	0.42 [m]
pelvic spring stiffness	1.2 [Nm/rad]
Foot contact yaw damping	0.1 [Nm s/rad]
Ankle actuation start angle	-0.08 [rad]
Ankle actuation final angle	0.2 [rad]

3. NUMERICAL SIMULATION

In this section we wish to describe the numerical procedures used. The simulations were performed with MATLAB.

The simulation is started when the stride is just beginning and both legs are momentarily on the ground. The hind leg is about to take off. The subsequent motion of the legs can now be found by numerically integrating the equations of motion describing the walker. The swing leg will at some point in time hit the ground again; the end of the stride. Assuming that this heel strike is inelastic, the foot will stay on the ground. The impact changes the velocities of each leg. Now, the model is poised to begin another stride. If speeds and angles at this instant are equal (but mirrored) to their values at the beginning of the previous stride, then the model has hit upon a passively re-entrant cycle and can theoretically keep walking indefinitely. If small errors are inserted in this cyclic motion, they could grow with each stride if the motion is unstable or decay, and eventually disappear over a number of strides if the motion is stable.

This section describes the numerical methods used to calculate the motion of the multibody system, to find initial conditions resulting in a cyclic walking motion and to determine the stability of that walking motion.

3.1 Equations of motion

First, we need to derive the Newton-Euler equations of motion for a multibody system, expressed in terms of independent coordinates. For each rigid body, there are three linear and three angular equations,

$$\begin{aligned} \Sigma \mathbf{f}^e &= m^e \ddot{\mathbf{x}}^e, \\ \Sigma \mathbf{T}^e &= \mathbf{J}^e \dot{\boldsymbol{\omega}}^e + \boldsymbol{\omega}^e \times \mathbf{J}^e \boldsymbol{\omega}^e \end{aligned} \tag{1}$$

with the global applied force vector $\mathbf{f}^e$, the body mass m^e, the applied torque vector $\mathbf{T}^e$, the inertia matrix $\mathbf{J}^e$, and the angular velocity vector $\boldsymbol{\omega}^e$, we expressed in the body fixed reference frame. All body contributions are added to a global mass matrix $\mathbf{M}$ and force vector $\mathbf{f}$. The unreduced equations of motion

$$\mathbf{M}(\mathbf{x})\ddot{\mathbf{x}} - \mathbf{f}(\dot{\mathbf{x}}, \mathbf{x}, t) = \mathbf{0} \tag{2}$$

are developed into an equation of virtual power,

$$\delta\dot{\mathbf{x}}^T(\mathbf{M}(\mathbf{x})\ddot{\mathbf{x}} - \mathbf{f}(\dot{\mathbf{x}}, \mathbf{x}, t)) = 0 \tag{3}$$

Here, $\delta\dot{\mathbf{x}}$ are kinematically admissible virtual velocities, which satisfy all instantaneous kinematic constraints. It is assumed that the coordinates, $\mathbf{x}$, depend on a number of independent generalized coordinates, $\mathbf{q}$, the kinematic degrees of freedom, by means of a transfer function $\mathbf{F}$ as

$$\mathbf{x} = \mathbf{F}(\mathbf{q}) \tag{4}$$

By differentiating this transfer function we obtain the kinematic admissible virtual velocities as

$$\delta\dot{\mathbf{x}} = \mathbf{F}_{,\mathbf{q}}\delta\dot{\mathbf{q}} \tag{5}$$

and the coordinate accelerations as

$$\ddot{\mathbf{x}} = \mathbf{F}_{,\mathbf{q}}\ddot{\mathbf{q}} + \mathbf{F}_{,\mathbf{qq}}\dot{\mathbf{q}}\dot{\mathbf{q}} \tag{6}$$

where we use the comma operator to denote partial derivatives:

$$\mathbf{F}_{,\mathbf{q}} = \frac{\partial \mathbf{F}}{\partial \mathbf{q}} \tag{7}$$

Substituting expressions (5) and (6) in the virtual power equation (3) yields the reduced equations

$$\overline{\mathbf{M}}\ddot{\mathbf{q}} = \overline{\mathbf{f}} \tag{8}$$

with the reduced mass matrix $\overline{\mathbf{M}}$ and force vector $\overline{\mathbf{f}}$ as

$$\overline{\mathbf{M}} = \mathbf{F}_{,\mathbf{q}}^T\mathbf{M}\mathbf{F}_{,\mathbf{q}}, \qquad \overline{\mathbf{f}} = \mathbf{F}_{,\mathbf{q}}^T[\mathbf{f} - \mathbf{M}\mathbf{F}_{,\mathbf{qq}}\dot{\mathbf{q}}\dot{\mathbf{q}}]. \tag{9}$$

Constructing the equations in this way provides a computationally efficient method.

3.2 Numerical integration

We now have a set of second order ordinary differential equations in the form of

$$\ddot{\mathbf{q}} = \mathbf{f}(\mathbf{q}, \dot{\mathbf{q}}, t) \tag{10}$$

For numerical integration we will use a scheme specially suitable for second order differential equations, as proposed by Meijaard.[12] This is a single step explicit integration scheme. For a given step size h, the integration error is in general $E = \mathcal{O}(h)$, and even $E = \mathcal{O}(h^2)$ if the system is very weakly dependent on $\dot{\mathbf{q}}$ (moderate velocities and weak damping). This is a very efficient integration scheme, compared to other methods like the classical fourth order Runge-Kutta method. The method calculates the positions and velocities at $t_{n+1} = t_n + h$ by evaluating the equations of motion *only once per integration step* at the estimated midpoint $t = t_n + \frac{1}{2}h$:

$$\begin{aligned} \mathbf{k}_n &= f(\dot{\mathbf{q}}_n, q_n + \tfrac{1}{2}h\dot{\mathbf{q}}_n, t_n + \tfrac{1}{2}h) \\ \mathbf{q}_{n+1} &= \mathbf{q}_n + h\dot{\mathbf{q}}_n + \tfrac{1}{2}h^2\mathbf{k}_n \\ \dot{\mathbf{q}}_{n+1} &= \dot{\mathbf{q}}_n + h\mathbf{k}_n \end{aligned} \tag{11}$$

https://doi.org/10.1017/S0263574700003040 Published online by Cambridge University Press

The maximum allowable step size to prevent numerical instability is characterized by

$$h_{max} = (1 - \beta)\frac{2}{\lambda_{max}} \tag{12}$$

with β the relative damping, and λ_{max} the largest undamped *eigenfrequency* of the linearised multibody system at its current state.

3.3 Rootfinding

In order to find the gait, the instant that heel strike occurs at the end of the stride has to be determined. This is detected by a change of sign in the swing foot clearance function $G_y(\mathbf{q})$ between the discrete moments in time t_n and t_{n+1},

$$G_y(\mathbf{q}(t_n))G_y(\mathbf{q}(t_{n+1})) < 0. \tag{13}$$

This zero crossing of $G_y(\mathbf{q}(t))$ can be found with the help of a bisection or a Newton-Raphson procedure. In any case we need to calculate intermediate values of $\mathbf{q}(t)$. A fast and accurate approach, as proposed by Meijaard,[13] is interpolating $\mathbf{q}$ between t_n and t_{n+1} with a third-order interpolation polynomial, since we know both $\mathbf{q}$ and $\dot{\mathbf{q}}$ at these instants

$$\mathbf{q}(t) = \begin{bmatrix} (1 - 3\xi^2 + 2\xi^3) \\ (\xi - 2\xi^2 + \xi^3)h \\ (3\xi^2 - 2\xi^3) \\ (-\xi^2 + \xi^3)h \end{bmatrix}^T \begin{bmatrix} \mathbf{q}(t_n) \\ \dot{\mathbf{q}}(t_n) \\ \mathbf{q}(t_{n+1}) \\ \dot{\mathbf{q}}(t_{n+1}) \end{bmatrix} \tag{14}$$

with $\xi = (t - t_n)/h$ and $h = t_{n+1} - t_n$. By simple interpolation and evaluation of the clearance function $G_y(\mathbf{q})$ the moment of heel contact can be calculated within any given error tolerance. We thus avoid evaluating the system equations (8) to find the zero crossing.

3.4 Impact equations

We assume that the heel strike behaves as a fully inelastic impact (no slip, no bounce), which is in accordance with observations on existing passive dynamic walking prototypes. Also, double stance is assumed to occur instantaneously. As soon as the swing foot hits the floor the stance foot lifts up, not interacting with the ground during impact. The resulting vertical velocity of the lifting foot should then be pointed upwards. If this is confirmed after the impact equations are solved, the assumption is verified. Otherwise, the robot would come to a complete stop.

Treating heel strike as an impact, we assume that velocities change instantaneously. These velocity jumps are enforced by very high values of the contact forces acting only during a small time interval of contact. In the limit case the first go to infinity and the second goes to zero. The integral of the force with respect to time over the duration of the impact, the impulse, has a finite value which is the cause of the velocity jump. while the impact takes place all positions as well as all non-impulsive forces of the multibody system remain constant.

The impact is usually divided into a compression and an expansion phase. Newton's impact law links these two phases by stating that the relative speed after impact equals e times the relative speed before impact but in opposite direction. The factor e is the coefficient of restitution. A value of $e = 1$ would correspond with a fully elastic impact whereas we use the value of $e = 0$, representing a completely inelastic impact and the two parts "stick" together after impact.

For a multibody system the reduced equations of motion (8) can be written in terms of the independent coordinates

$$\overline{\mathbf{M}}\ddot{\mathbf{q}} = \bar{\mathbf{f}} \tag{15}$$

with the reduced mass matrix $\overline{\mathbf{M}}$, the accelerations of the generalized coordinates $\ddot{\mathbf{q}}$ and the reduced force vector $\bar{\mathbf{f}}$. Note that the "lifting stance foot"-assumption implies that the system has more degrees of freedom during impact than during smooth motion. When contact occurs, the former swing foot becomes constrained and the equations of motion become

$$\overline{\mathbf{M}}\ddot{\mathbf{q}} + \mathbf{G}_{,\mathbf{q}}^T\boldsymbol{\lambda} = \bar{\mathbf{f}} \tag{16}$$

with the contact forces $\boldsymbol{\lambda}$ dual to the relative contact velocities $\dot{G}_x$, $\dot{G}_y$ and $\dot{G}_z$. Integration of these equations of motion over the time of impact and taking the limit case yields

$$\lim_{t^- \uparrow t^+} \int_{t^-}^{t^+} (\overline{\mathbf{M}}\ddot{\mathbf{q}} + \mathbf{G}_{,\mathbf{q}}^T\boldsymbol{\lambda})dt = 0. \tag{17}$$

The total force vector $\bar{\mathbf{f}}$ only contains nonimpulsive forces and therefore the right-hand side vanishes. Under the introduction of the contact impulse,

$$\boldsymbol{\rho} = \lim_{t^- \uparrow t^+} \int_{t^-}^{t^+} \boldsymbol{\lambda} dt, \tag{18}$$

and noting that the mass matrix stays constant during impact, the momentum equations for the multibody system become

$$\overline{\mathbf{M}}\dot{\mathbf{q}}^+ + \mathbf{G}_{,\mathbf{q}}\boldsymbol{\rho} = \overline{\mathbf{M}}\dot{\mathbf{q}}^- \tag{19}$$

with $\dot{\mathbf{q}}^-$ the velocities before and $\dot{\mathbf{q}}^+$ the velocities of the system after impact. Together with Newton's impact law,

$$\dot{\mathbf{G}}^+ = -e\dot{\mathbf{G}}^- \quad \Rightarrow \quad \mathbf{G}_{,\mathbf{q}}\dot{\mathbf{q}}^+ = -e\mathbf{G}_{,\mathbf{q}}\dot{\mathbf{q}}^- \tag{20}$$

we have a complete linear set of equations for solving the velocities after impact, $\dot{\mathbf{q}}^+$, together with the contact impulse $\boldsymbol{\rho}$. Taking (19) and (20) together, the complete set of impact equations reads

$$\begin{bmatrix} \overline{\mathrm{M}} & \mathbf{G}_{,\mathbf{q}}^T \\ \mathbf{G}_{,\mathbf{q}} & \mathbf{0} \end{bmatrix} \begin{bmatrix} \dot{\mathbf{q}}^+ \\ \boldsymbol{\rho} \end{bmatrix} = \begin{bmatrix} \mathbf{M}\dot{\mathbf{q}}^- \\ -e\mathbf{G}_{,\mathbf{q}}\dot{\mathbf{q}}^- \end{bmatrix} \tag{21}$$

With one impact occurring at a time these equations can be solved.

After the post-impact velocities are calculated, we mirror the state of the walker with respect to the sagittal plane (= symmetry plane) in order to compare this with the initial state.

https://doi.org/10.1017/S0263574700003040 Published online by Cambridge University Press

3.5 Periodic solutions

With the above procedure (numerically integrating equations of motion, impact-detection and calculation and left-rightly mirroring) the initial conditions $\mathbf{v} = (\dot{\mathbf{q}}, \mathbf{q})$ can be mapped from one stride onto the next. McGeer[14] introduced the 'stride function'

$$\mathbf{v}_{n+1} = \mathbf{S}(\mathbf{v}_n) \tag{22}$$

A walking cycle is specified by the requirement that the vector of initial conditions $\mathbf{v}_n$ results in identical initial conditions for the subsequent stride:

$$\mathbf{v}_{n+1} = \mathbf{v}_n \tag{23}$$

A vector with initial conditions satisfying this requirement is a cyclic solution $\mathbf{v}_c$, which maps onto itself:

$$\mathbf{S}(\mathbf{v}_c) = \mathbf{v}_c \tag{24}$$

A cyclic solution can be found by a linearization of the stride function

$$\begin{aligned} \mathbf{S}(\mathbf{v}+\Delta\mathbf{v}) &\approx \mathbf{S}(\mathbf{v}) + \mathbf{J}\Delta\mathbf{v} \\ \textit{with}\ \ \mathbf{J} &= \tfrac{\partial \mathbf{S}}{\partial \mathbf{v}} \end{aligned} \tag{25}$$

and applying a Newton-Raphson iteration procedure, starting with a set of initial conditions $\mathbf{v}$ close to the cyclic solution $\mathbf{v}_c$

repeat

$$\begin{aligned} \Delta\mathbf{v} &= [\mathbf{I} - \mathbf{J}]^{-1}(\mathbf{S}(\mathbf{v}) - \mathbf{v}) \\ \mathbf{v} &= \mathbf{v} + \Delta\mathbf{v} \end{aligned} \tag{26}$$

until $|\Delta\mathbf{v}| < \varepsilon$

where $\mathbf{I}$ is the identity matrix. The Jacobian $\mathbf{J}$ is calculated by a perturbation method, which involves simulation of a full walking stride for every initial condition. The result of this depends on the model parameters and the initial estimate for the solution. If the parameters are such that no cyclic gait exists or if the initial estimate is poor, then the solution will diverge. If the solution converges we find one of possibly multiple cyclic solutions. McGeer[14] and Garcia[15] showed that with their 2D walkers there usually exist two cyclic solutions, one with a longer stride than the other. The long-period solution tends to be more stable than the short-period solution. We always found only the long-period solution, most likely meaning that this more stable solution is much easier obtained by the Newton-Raphson iteration than the short-period solution.

3.6 Stability

If the walker starts a stride exactly with $\mathbf{v}_c$, it will walk forever. However, if small errors $\boldsymbol{\epsilon}_n$ appear, the periodic solution needs to be stable for the robot to maintain gait. The stability is described with the Jacobian $\mathbf{J}$ from the previous subsection, which is the linearised multiplication factor for errors from one stride to the next:

$$\mathbf{v}_c + \boldsymbol{\epsilon}_{n+1} = \mathbf{S}(\mathbf{v}_c + \boldsymbol{\epsilon}_n) = \mathbf{S}(\mathbf{v}_c) + \mathbf{J}\boldsymbol{\epsilon}_n + \mathcal{O}(\boldsymbol{\epsilon}_n^2) \tag{27}$$

Errors will asymptotically die out if all *eigenvalues* of the stride function Jacobian $\mathbf{J}$ have an absolute value smaller than 1, and in that case the periodic solution is stable.

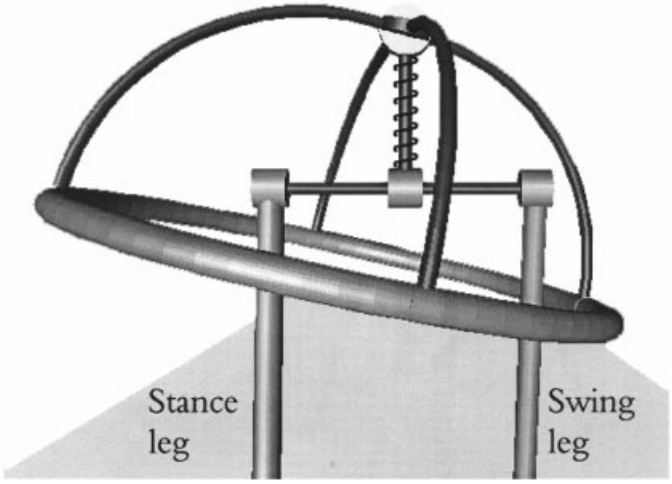


Fig. 10. The compensator body acts as an unactuated pendulum in the frontal plane, preventing the walker from tipping over sideways.

Finding a stable solution by varying the parameter values 'by hand' is usually pretty easy for the 2D walkers. This process can also be optimized with a searching algorithm, but this tends to be problematic, both regarding the computation time needed and slow convergention if any.

4. RESULTS

Our main question is: will a 3D passive dynamic walker with a dynamic compensator for the yaw and roll motions be inherently stable? We will first show the stability results for a 2D version of our model. Then, we will show that the 3D version is not stable, unless compensated with the pelvic body. The design parameters have not been numerically optimized; this falls outside the scope of our research. We manually tuned the parameters until we found a stable configuration (see Table I).

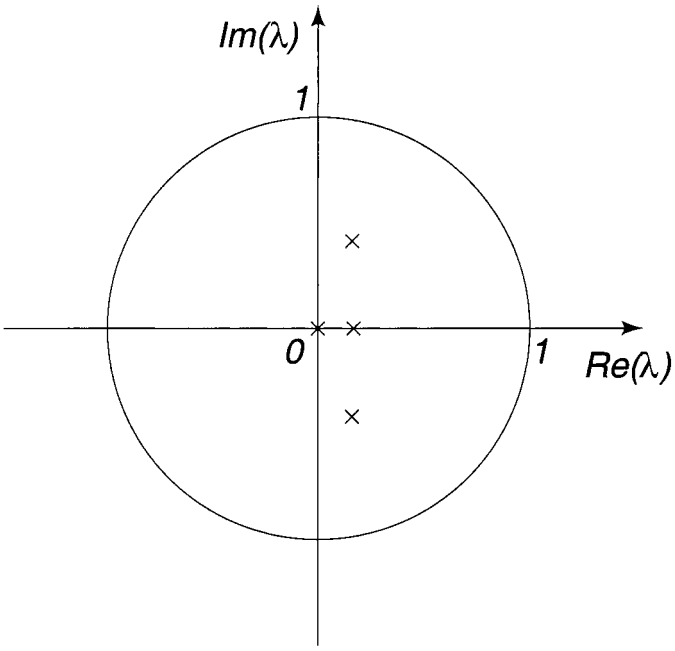


Fig. 11. Stability of the 2D version of our complete model: a 2D, kneed walker with actuated ankles.

https://doi.org/10.1017/S0263574700003040 Published online by Cambridge University Press

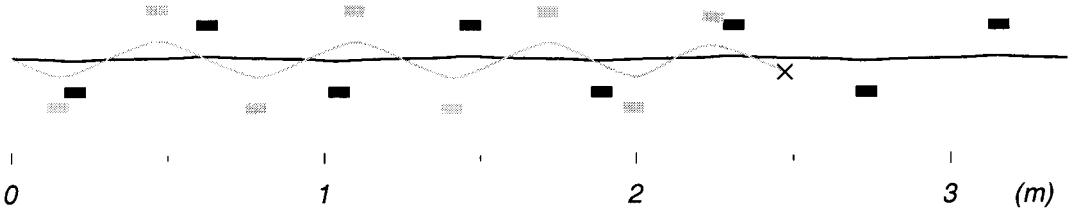


Fig. 12. Projection of the path of the center of mass on the floor. Without compensation (gray), the zigzag walking motion fails after eight steps. With a pelvic compensator (black) the robot walks straight and stably.

One of the main reasons for working with the concept of Passive Dynamic Walking is to achieve an energy-efficient machine. Our highly underactuated walking machine (two partially actuated ankle joints for a system with nine degrees of freedom) with a total mass of about 3 kg used 0.15 Joule/kg m at a nominal speed of 0.5 m/s. This approximately equals the energy input into the passive dynamic walkers of McGeer and Garcia that walk down a slope of about 1 degree.

4.1 Stability of 2D version

McGeer found that both his simple straight-legged 2D walker and his robot with knees had a fairly large range of parameter values resulting in stability.[14] These results have been experimentally proven by several working prototypes.

We performed simulations of a 2D version of our compensated 3D model, involving knees and ankles, but no yaw and roll motions. Figure 11 shows the *eigenvalues* of the Jacobian of the stride function **J** (27) represented in the complex plane. The walker is stable when all *eigenvalues* are situated within the unit circle.

The *eigenvalues* lie well within the unit circle. This shows that the 2D version of our walker has an applicable level of inherent stability, comparable to that of McGeer's and Garcia's working prototypes.

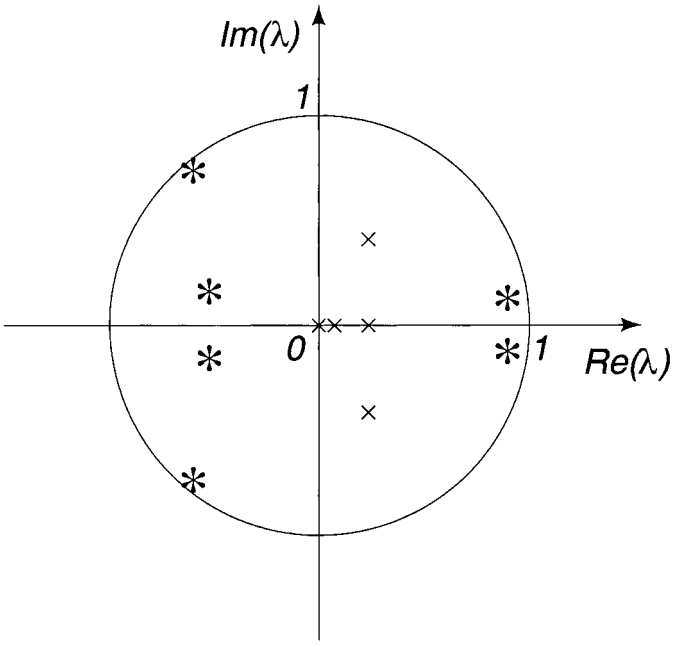


Fig. 13. Stability of the semi-3D model with a yaw compensator. The * indicates the extra *eigenvalues* from the extension of the 2D version to the 3D model with a pelvic compensator body.

4.2 3D model

The extension from 2D to 3D involves the extra abilities for the robot to yaw and to roll. Figure 12 shows the path of the center of the hip-axle projected on the floor, once with and once without the presence of a pelvic compensator body. With the pelvic compensator, the robot walks nearly in a straight line, demonstrating successful compensation of the yaw-motion. The non-compensated model not only walks in a zigzag, but is also unstable. The yaw motion increases slightly each stride, influencing the forward motion of the legs until the robot fails by falling backward or making heel contact too early.

This shows that the pelvic compensator successfully eliminates the undesired 3D motions, so that the legs practically move as if in a 2D environment. This also has a positive effect on the stability of the 3D walker. Figure 13 shows the *eigenvalues* of the manually tuned 3D model with pelvic body, which are all inside the unit circle. The *eigenvectors* belonging to the six *eigenvalues* closest to the unit circle mostly show the yaw and roll motions of the legs and the pelvic body. This can also be deduced from comparison of this figure with the stability plot of the 2D version (Figure 11). Note that the extension of the 2D walker with 3D motions not only introduces new *eigenvalues*, but also slightly changes the numerical values of the previously existing *eigenvalues*.

5. CONCLUSION

A 3D passive dynamic walker can be successfully compensated with the aid of a pelvic compensator body mounted on the hip-axle. The extra 3D motions, yaw and roll, are shifted from the legs to the pelvic body, so that the robot walks in a straight line, without falling over sideways. This nearly 2D leg motion results in a stable cyclic walking motion.

Our research shows that a 3D passive dynamic walker can be stable. However, the *eigenvalues* as presented here are still quite close to the unit circle, the boundary to instability. Our future research will aim at finding a more robust 3D model, followed by the construction of a prototype.

The choice of foot contact model is a very important factor for the outcome of the simulations, and should receive a detailed study.

The interaction of the different 3D motions exponentially increases the complexity of the model behaviour. Understanding the characteristics of 3D passive dynamic walkers

https://doi.org/10.1017/S0263574700003040 Published online by Cambridge University Press

will allow us to apply this energy-efficient concept in real-world applications.

Acknowledgements
This work was supported by the Dutch Technology Foundation STW, grant DWT4551. Thanks to Andy Ruina for many helpful comments.

References

1. K. Hirai, M. Hirose, Y. Haikawa and T. Takenaka, "The development of Honda humanoid robot" *Proc. IEEE International Conference on Robotics and Automation* (May, 1998) pp. 1321–1326.
2. T. McGeer, "Passive dynamic walking" *Intern. J. Robot. Res.* **9**, 62–82 (April, 1990).
3. S. Mochon and T.A. McMahon, "Ballistic walking" *J. Biomechan.* **13**, 49–57 (1980).
4. M. Garcia, A. Chatterjee and A. Ruina, "Speed, efficiency, and stability of small-slope 2D passive-dynamic bipedal walking" *Proc. IEEE International Conference on Robotics*, Piscataway, NJ (1998) pp. 2351–2356.
5. B. Bechstein and P.O. Uhlig, "Walking toy ('improvements in and relating to toys')", *U.K. Patent*, No. 7453 (December 5, 1912).
6. T. McGeer, "Passive walking with knees" *Proc. 1990 IEEE International Conference on Robotics and Automation*, Los Alamitos, CA (1990) pp. 1640–1645.
7. M.J. Coleman and A. Ruina, "An uncontrolled toy that can walk but cannot stand still" *Physical Review Letters* **80**, 3658–3661 (April, 1998).
8. R.Q. vd. Linde, "Ontwerpen van een tweebenige looprobot (Design of a biped)" *Master's thesis* (Delft University of Technology, Delft, The Netherlands, 1995). Report A-726.
9. J. Adolfsson, H. Dankowicz, and A. Nordmark, "3D passive walkers, finding periodic gaits in the presence of discontinuities" (to appear in Nonlinear Dynamics, 2000).
10. R.Q. vd. Linde, "Active leg compliance for passive walking" *Proc. IEEE International Conference on Robotics and Automation* (May, 1998) pp. 2339–2344.
11. A.D. Kuo, "Stabilization of lateral motion in passive dynamic walking" *Int. J. Robot. Res.* **18**, 917–930 (September, 1999).
12. J.P. Meijaard, "A comparison of numerical integration methods with a view to fast simulation of mechanical dynamical systems" *Real-Time Integration Methods for Mechanical System Simulation* **69**, 329–343 (1990) NATO ASI Series F: Computer and Systems Sciences.
13. J.P. Meijaard, "Efficient numerical integration of the equations of motion of non-smooth mechanical systems" *Zeitschr. der Angew. Math. Mech.* **77**, No. 6, 419–427 (1997).
14. T. McGeer, "Passive dynamic biped catalogue" *Proc. Experimental Robotics II: The 2nd International Symposium* (R. Chatila and G. Hirzinger, eds.), (Springer, Berlin, 1999), pp. 465–490.
15. M. Garcia. A. Chatterjee, A. Ruina and M.J. Coleman, "The simplest walking model: Stability, complexity, and scaling" *ASME J. Biomech. Eng.* **120**, 281–288 (April, 1998).

https://doi.org/10.1017/S0263574700003040 Published online by Cambridge University Press